Combinatorial Optimization of the DNA Cleaving Ni(II)·Xaa-Xaa-His Metallotripeptide Domain†

Xiaofen Huang, Mary E. Pieczko, and Eric C. Long*

Department of Chemistry, Purdue University School of Science, Indiana University Purdue University-Indianapolis, Indianapolis, Indiana, 46202-3274

Received October 29, 1998; Revised Manuscript Received December 11, 1998

ABSTRACT: A positional-scanning combinatorial protocol was employed to optimize the deoxyribose-based cleavage of B-form DNA by Ni(II)·Xaa-Xaa-His metallopeptides. This procedure employed 18 naturally occurring amino acids (excluding Cys and Trp) to generate two libraries in which the first and second positions of the peptide ligand were varied. Increased direct DNA cleavage relative to Ni(II)·Gly-Gly-His was observed when (1) the amino-terminal peptide position contained Pro, Met, Arg, or Lys (with Pro exhibiting the greatest activity) and (2) the second peptide position contained Lys, Arg, Met, Ser, or Thr (with Lys exhibiting the greatest activity); the optimized metallopeptide, Ni(II)·Pro-Lys-His, was found to cleave DNA an order of magnitude better than Ni(II)·Gly-Gly-His. While metal complexation and the A/T-rich site selectivity of the optimized metallopeptides were not altered, DNA binding affinity was slightly increased relative to Ni(II)·Gly-Gly-His, however, not to an extent necessary to account for the observed increase in reactivity. Examination of molecular models of Ni(II)·Pro-Lys-His bound to the minor groove of DNA via hydrogen bonding of the His N3 imidazole hydrogen to the N3 of adenine or O2 of thymine suggests that the Pro residue can make hydrophobic contacts with the sugars lining the walls of the groove while the Lys residue is able to form a salt bridge with a proximal phosphate; with these interactions, the metal center is poised to abstract the C4′-H of an adjacent nucleotide suggesting that noncovalent interactions result in a positioning which contributes to increased DNA cleavage activity.

Metallopeptides of the general form Ni(II)·Xaa-Xaa-His[1] are finding increased utility in the biochemical analysis of protein−nucleic acid and protein−protein interactions in solution (*1*−*3*). This metallotripeptide domain, which is based on the amino-terminal, square-planar Cu(II) and Ni(II) chelating domain of serum albumins (Figure 1) (*2*), can be synthetically (*1*−*4*) or biosynthetically (*5*) appended to proteins or other agents and, when appropriately activated, allows a modified agent to affinity cleave or oxidatively modify a noncovalently associated macromolecule through the generation of a nondiffusible oxidizing equivalent (*1*−*3*). Experiments employing Ni(II)·Xaa-Xaa-His domains have revealed details of the site selectivity and orientation of intermolecular binding interactions in proximity to the appended metallopeptide domain; recent examples involving the use of Ni(II)·Xaa-Xaa-His-modified biomolecules have examined the following: protein-DNA (*5*−*9*) and PNA-DNA (*10*) interactions through affinity cleavage; protein−protein interactions through oxidative cross-linking (*11*−*13*); directed protein cleavage by low molecular weight agents (*14*); and small molecule−nucleic acid interactions (*15*, *16*). Clearly, this range of applications suggests that understanding the chemical reactivity of Ni(II)·Xaa-Xaa-His domains and structural features which may improve their activity could facilitate the further understanding of macromolecular interactions.

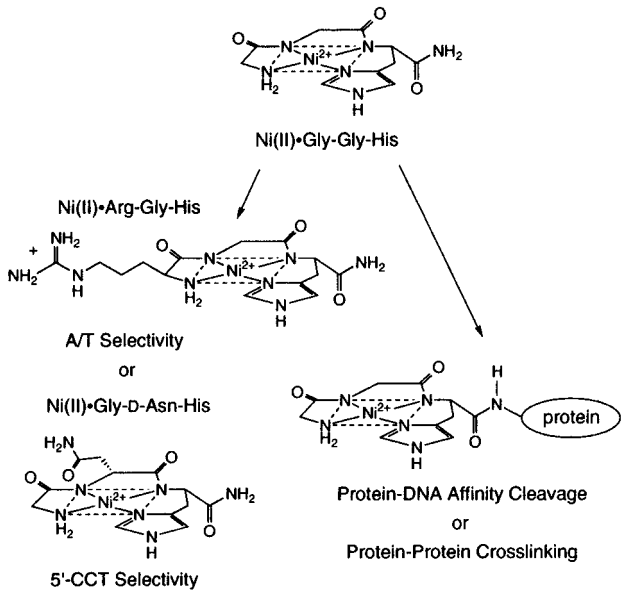

FIGURE 1: Representative Ni(II)·Xaa-Xaa-His metallopeptides and derivatives active in nucleic acid and protein modification experiments.

† This research was supported by a grant from the National Institutes of Health (GM50557).

* To whom correspondence should be addressed at the Department of Chemistry, Indiana University Purdue University-Indianapolis, 402 North Blackford Street, Indianapolis, IN 46202-3274. E-mail: long@chem.iupui.edu. Tel: (317) 274-6888. Fax: (317) 274-4701.

[1] Abbreviations: FAB-MS, fast atom bombardment-mass spectrometry; MMPP, magnesium monoperoxyphthalate; Oaa, specifically defined α-amino acid; OAc, acetate; PNA, peptide nucleic acid; Xaa, α-amino acid; TFA, trifluoroacetic acid; TFMSA, trifluoromethanesulfonic acid.

10.1021/bi982587o CCC: $18.00
Published on Web 01/29/1999

In addition to their use in the modification of existing proteins and other agents, Ni(II)·Xaa-Xaa-His metallopeptides are currently being examined by our laboratory as stand-alone agents to further the understanding of peptide− and amino acid−nucleic acid recognition principles (*3*, *17*−*19*). Ni(II)·Xaa-Xaa-His metallopeptides (where Xaa-Xaa-His is NH_2-Xaa-Xaa-His-$CONH_2$ and Xaa is an α-amino acid) can be activated to selectively degrade DNA through C4′−H abstraction via a minor groove binding interaction (*17*, *19*). This initially formed deoxyribose-based lesion results in direct DNA strand scission or alkaline-labile site formation (*19*); we have demonstrated previously that site-selective DNA cleavage via C4′−H abstraction is dependent upon the composition and chirality of the amino acids included in the Xaa-Xaa-His ligand (Figure 1) (*17*). In addition, recent results indicate that Ni(II)·Xaa-Xaa-His metallopeptides can oxidatively modify guanine nucleobases under appropriate conditions (*19*, *20*) and selectively cleave RNA loop regions (*21*). Overall, given their use of amino acids, Ni(II)·Xaa-Xaa-His metallopeptides are unique in their ability to incorporate and position within a metal complex framework the same chemical functionalities (e.g., guanidinium, amide, or amine moieties) used by proteins, natural products, and antitumor agents for the molecular recognition of DNA and RNA. These features, therefore, make Ni(II)·Xaa-Xaa-His metallopeptides attractive models to further our understanding of peptide or protein nucleic acid recognition principles especially as they relate to the specific interactions which occur between peptide moieties and the minor groove of DNA.

To systematically explore alternative amino acid compositions of the Ni(II)·Xaa-Xaa-His metallopeptide domain leading to increased levels of direct, deoxyribose-based C4′−H abstraction, we have utilized a positional-scanning combinatorial procedure (*22*, *23*) employing naturally occurring L-α-amino acids to produce a library of alternative, biosynthetically accessible amino acid compositions at both Xaa positions of Ni(II)·Xaa-Xaa-His. Herein we describe the combinatorial modification of the basic Ni(II)·Xaa-Xaa-His domain to determine the amino acid composition which optimizes the deoxyribose-based, B-form DNA cleavage reaction. Importantly, these findings (1) impact the use of Ni(II)·Xaa-Xaa-His domains in synthetic or biosynthetic protein modification protocols and (2) reveal interesting amino acid configurations within the Ni(II)·Xaa-Xaa-His framework that facilitate minor groove recognition and cleavage by these metallopeptides. While the model system described herein seeks to customize the Ni(II)·Xaa-Xaa-His tripeptide for interaction with B-form DNA, this same synthetic protocol can be used or expanded to optimize the Ni(II)·Xaa-Xaa-His domain for applications in protein−nucleic acid and protein−protein interactions.

EXPERIMENTAL PROCEDURES

Materials. All protected amino acids were purchased from Bachem California. Plasmid DNA substrates (φX174 RF and pBR322) were purchased from GIBCO Life Technologies, Inc. [α-^{32}P]dATP and [γ-^{32}P]ATP were obtained from NEN-Dupont. All other reagents and enzymes were obtained in the highest grades commercially available. All buffers were prepared using Milli-Q purified water.

Synthesis of Xaa-Xaa-His Libraries. Two synthetic peptide combinatorial libraries derived from the basic Xaa-Xaa-His sequence were synthesized using standard *t*-Boc protocols on methylbenzhydrylamine (mBHA) resin to yield tripeptides having free amino-termini and amidated carboxy-termini (*24*). The two peptide libraries generated, Oaa_1-Xaa-His and Xaa-Oaa_2-His [where Oaa is a specifically defined L-α amino acid (excluding Cys and Trp) and Xaa is any one of 18 naturally occurring L-α amino acids (excluding Cys and Trp)] (*22*, *23*), were prepared using a resin split-and-mix procedure and a simple apparatus for manually conducting multiple parallel solid-phase syntheses in fritted glass vials (*25*).

In a typical preparation of the Oaa_1-Xaa-His library, 1.8 g (1.44 mmol) of His-substituted mBHA resin was divided equally among 18 different vials and coupled to one of 18 naturally occurring L-amino acids. Upon completion of this amino acid coupling step, the 18 different dipeptide resins contained in these vials were recombined, mixed, and redistributed among 18 clean vials for the final coupling to a defined (Oaa_1) amino acid. Following TFA side chain deprotection, the peptides were cleaved from the resin using TFMSA (*24*) yielding 18 different tripeptide mixtures where the amino-terminal position is defined (Oaa_1) and the second position contains one of 18 different L-amino acids (Xaa). Alternatively, to generate the Xaa-Oaa_2-His library, 6.5 g of His-substituted mBHA resin was divided into 18 individual vials and coupled to one of 18 different, defined amino acids. Each of the 18 different dipeptide resins generated (Oaa_2-His) was further divided among 18 fresh vials and again coupled to one of 18 different amino acids. After this second amino acid coupling step, the contents of the 18 vials for a particular Oaa_2 group were recombined and deprotected, as described above, to produce one member of the Xaa-Oaa_2-His library; this procedure was repeated to generate the remaining 17 peptide mixtures that make up the total Xaa-Oaa_2-His library. The compositions of the resulting Oaa_1-Xaa-His and Xaa-Oaa_2-His libraries were quantitated and verified by amino acid analysis to contain equivalent representation of all amino acids used.

Cleavage of Supercoiled Plasmid DNA. The relative cleavage efficiencies of the Oaa_1-Xaa-His and Xaa-Oaa_2-His libraries were determined by preincubating peptides with one equivalent of $Ni(OAc)_2$ in 10 mM sodium cacodylate buffer (pH 7.5) for 10 min, followed by the addition of φX174 RF plasmid DNA (11 μM base pair concentration) in a total volume of 20 μL. Cleavage reactions were initiated upon addition of one equivalent of $KHSO_5$ (based on metallopeptide) to complete the final volume and quenched after 1.0 min with an EDTA-containing loading buffer. Reactions were analyzed on 0.9% agarose gels containing ethidium bromide which were electrophoresed at 60 V for 2 h and visualized using a UV transilluminator.

DNA cleavage quantitation of the above gels was performed through photoimaging densitometry of each lane using an IPLab Gel™ software program interfaced to a Macintosh computer. Quantitation of DNA cleavage was performed by dividing the total quantitated amount of form II produced in each reaction by the total amount of DNA present; a correction factor of 1.42 was multiplied to the values obtained for form I DNA to adjust for differential ethidium bromide staining (*26*).

Cleavage of ^{32}P-End-Labeled DNA. End-labeled restriction fragments were prepared (*27*) by digesting supercoiled pBR322 plamid DNA with *Eco*RI restriction endonuclease followed by 3′-end labeling with terminal deoxynucleotidyl transferase and [α-^{32}P]dATP. Alternatively, 5′-end labeling was achieved by sequential treatment of *Eco*RI-treated DNA with alkaline phosphatase, [γ-^{32}P]ATP, and T4 polynucleotide kinase. Upon incorporation of label, the DNA was further digested with *Rsa*I to yield ^{32}P-end-labeled 167 and 514 base pair fragments that were purified by 6% preparative nondenaturing gel electrophoresis and isolated by electroelution.

Metallopeptide-induced cleavage reactions were carried out in 20 μL total volumes containing calf thymus DNA (50 μM nucleotide concentration) and 3×10^4 cpm of a ^{32}P-end-labeled restriction fragment in 10 mM cacodylate buffer (pH 7.5). Reactions were initiated through the admixture of DNA and equivalent amounts of preformed Ni(II)·peptide and $KHSO_5$. Reaction mixtures were quenched after 1.0 min with the addition of 3 μL of a 0.2 M EDTA solution, EtOH precipitated, and dried. The resulting DNA pellets were resuspended in 3 μL of an 80% formamide loading buffer. All reaction mixtures, along with Maxam−Gilbert G + A and T + C sequencing reaction mixtures (*27*), were heat denatured at 90 °C for 5 min and quick-chilled on ice. The samples were loaded onto 15% or 20% (19:1) polyacrylamide/7.5 M urea sequencing gels and electrophoresed at 1500 V for 8 h. Following electrophoresis, the gels were transferred to an autoradiography cassette and stored at −70 °C with Kodak X-omat film.

Determination of Binding Affinities. Metallopeptide−DNA binding constants were determined using ϕX174 RF DNA and distamycin as a competitive binding agent. The concentration of distamycin was determined optically using $\epsilon_{302} = 3.4 \times 10^4$ M^{-1} cm^{-1}. Reactions containing fixed amounts of Ni(II)·peptide were incubated with 11 μM (base pair concentration) of ϕX174 RF DNA in the presence of increasing amounts of distamycin. All other reaction conditions and quantitation procedures were identical to those employed in the supercoiled DNA cleavage reactions described previously. The binding constant of the Ni(II)·peptides were determined using published procedures (*28*) when 50% of the cleavable DNA was protected by distamycin (Supporting Information). The apparent binding constants were calculated from: $K_{\text{distamycin}}$[distamycin] = K_{app}[Ni(II)·peptide] where $K_{\text{distamycin}} = 10^8$ M^{-1} (*29*).

Molecular Modeling. Molecular modeling was performed on a Silicon Graphics workstation using Quanta CHARMm software. The structures of the Ni(II)·peptides were obtained through amino acid side chain modification of the crystal structure of Cu(II)·Gly-Gly-His (*30*). B-form DNA structures were created using the built-in nucleic acids builder program. The binding of metallopeptides to the minor groove of the DNA helix was achieved using the solid docking program which prevented the violation of van der Waals radii.

RESULTS AND DISCUSSION

Peptide Library Syntheses. Two peptide libraries derived from the basic Xaa-Xaa-His sequence were synthesized using standard *t*-Boc protocols to include all possible combinations of 18 naturally occurring L-α amino acids excluding Cys and Trp within the variable positions of the Xaa-Xaa-His peptide ligand; Cys and Trp were not included in the library syntheses to prevent disulfide formation and the partial DNA intercalation (*31*) of these residues, respectively. These libraries included (1) Oaa_1-Xaa-His and (2) Xaa-Oaa_2-His where the Oaa amino acid is specifically defined and Xaa can be any one of 18 naturally occurring amino acids. These libraries allow a positional scanning strategy to be employed in correlating amino acid composition to metallopeptide-induced DNA cleavage activity. Importantly, all libraries were examined by quantitative amino acid analysis to verify the uniform representation of all amino acids included in the library syntheses (e.g., the Ala-Xaa-His group was verified to contain a 19:19:1 ratio of Ala:His:all other amino acids included in the synthesis).

DNA Cleavage Efficiency. The DNA cleavage efficiencies of the individual members of the Oaa_1-Xaa-His and Xaa-Oaa_2-His libraries were examined through their ability to mediate the direct conversion of supercoiled plasmid (form I) DNA to nicked-circular (form II) DNA (as $KHSO_5$- or MMPP-activated Ni(II) complexes) (Supporting Information). This assay acts as a sensitive monitor of the C4′-H abstraction ability of these metallopeptides resulting in direct DNA strand scission via a minor groove binding interaction (*19*).

As shown in Figure 2, panel A, DNA cleavage efficiency by the Ni(II)·Oaa_1-Xaa-His family of metallopeptides is dependent upon the identity of the amino acid found at the amino-terminal peptide position. DNA cleavage by these metallopeptides was enhanced between 5- and 8-fold relative to our standard, Ni(II)·Gly-Gly-His, when Arg (R), Lys (K), Met (M), or Pro (P) was present in the amino-terminal peptide position. In contrast, the remaining amino acids incorporated at the defined Oaa_1 position of this library maintained a cleavage ability that was either similar to Ni(II)·Gly-Gly-His or slightly reduced in comparison to this "unmodified" metallotripeptide.

In addition to determining the amino acids which influence direct DNA cleavage activity at the amino-terminal position, we performed an identical experiment with the Ni(II)·Xaa-Oaa_2-His family of metallotripeptides to identify those amino acids which increase activity at the second position within the tripeptide ligand. As shown in Figure 2, panel B, plasmid DNA cleavage was enhanced 3−5-fold relative to Ni(II)·Gly-Gly-His when Oaa_2 was Arg, Lys, Met, Ser (S), or Thr (T); as observed with the Ni(II)·Oaa_1-Xaa-His library, other amino acids incorporated into this position exhibited an activity that was either similar or slightly reduced in comparison to Ni(II)·Gly-Gly-His.

The findings presented above identify the naturally occurring L-α amino acids, among the 18 employed, which increase the direct DNA strand scission activity of the basic Ni(II)·Xaa-Xaa-His metallopeptide framework and allow the rank ordering of their influence. In the case of the amino-terminal peptide position (Oaa_1), Pro > Met > Arg > Lys, while within the second peptide position (Oaa_2), Lys > Arg > Met/Ser/Thr. Importantly, these results (1) predict that Ni(II)·Pro-Lys-His would substantially increase the direct strand scission of B-form DNA in comparison to Ni(II)·Gly-Gly-His and (2) allow a quantitative and qualitative visualization of the effect of various amino acid placements and chemical functionalities within the Ni(II)·Xaa-Xaa-His framework on B-form DNA cleavage.

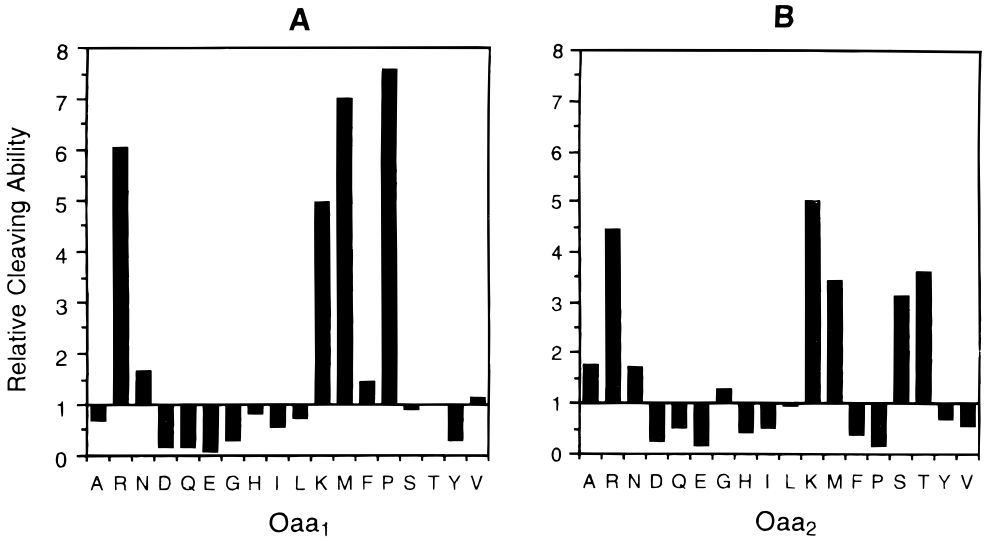

FIGURE 2: Quantitation of plasmid DNA cleavage activity by the Ni(II)·Oaa_1-Xaa-His and Ni(II)·Xaa-Oaa_2-His libraries relative to Ni(II)·Gly-Gly-His. The horizontal axis of each histogram represents the identity of the defined Oaa_1 or Oaa_2 amino acids present in each tripeptide (single letter amino acid code) while the vertical axis indicates the relative cleavage ability of 5 μM metallopeptide in comparison to 5 μM Ni(II)·Gly-Gly-His (bars at 1 indicate a cleavage ability identical to that of Ni(II)·Gly-Gly-His, bars above 1 indicate an *n*-fold increase in relative activity, and bars below 1 indicate the amount of decreased relative activity in the amount of the deflection from 1): panel A, plasmid DNA cleavage activity of the Ni(II)·Oaa_1-Xaa-His library; and panel B, plasmid DNA cleavage activity of the Ni(II)·Xaa-Oaa_2-His library.

To address the first point listed above, we prepared the peptide Pro-Lys-His independently and examined the DNA cleavage activity of its Ni(II) complex; plasmid DNA cleavage by this metallopeptide was found to be increased by greater than an order of magnitude in comparison to Ni(II)·Gly-Gly-His (data not shown) indicating an approximately additive effect of the two amino acid substitutions employed. Additional characterization of this complex, or Ni(II)·Pro-Gly-His, through metal ion titrations indicated the formation of 1:1 complexes that exhibit the same spectroscopic characteristics (Cu: $\lambda_{max} = 525$ nm; $\epsilon \sim 102$ cm^{-1} M^{-1}; Ni: $\lambda_{max} = 420$ nm; $\epsilon \sim 120$ cm^{-1} M^{-1}, Supporting Information) as other well-characterized Xaa-Xaa-His metallopeptides (*2*). These observations suggest the formation of a similarly, if not identically, structured complex in comparison to the Ni/Cu complexes of Gly-Gly-His.

With regards to the second point mentioned above, it appears that the positively charged amino acids Lys and Arg can favorably influence the minor groove-mediated direct strand scission of DNA in either the first or second positions of the metallopeptide, with a slight enhancement of activity exhibited by Arg in the first position relative to its placement in the second peptide position; the above results can be attributed to an increased electrostatic anchoring of the metallopeptide to the polyanionic DNA as indicated in previous experiments (*17*). Surprisingly, however, the above results also indicate that Pro, in addition to positively charged amino acids, can further increase metallopeptide activity when located in the first peptide position but, as expected given its structure, not the second position. In addition, analysis of the libraries also indicates that a Met residue located at either the first or second peptide position enhanced DNA cleavage activity, albeit with increased influence when located in the amino-terminal position. Along with these amino acid substitutions, Figure 2, panel B, indicates that amino acids containing a side chain alcohol functionality (Ser and Thr) can increase metallopeptide activity when included only at the second position of the peptide ligand. Curiously, most of the amino acids found to influence the minor groove interaction of the metallotripeptides leading to enhanced DNA cleavage are also those found in several important classes of minor groove binding protein motifs [e.g., the repeating Ser-Pro-Lys/Arg-Lys/Arg motifs of sea urchin histones H1 and H2B (*32*)]. These results suggest that the activity of the Ni(II)·Gly-Gly-His metallopeptides may be influenced by, and perhaps serve to model, the same fundamental amino acid−minor groove interactions that nature has chosen to employ in protein−DNA minor groove recognition events.

The above results, however, do not address whether the metallopeptide−DNA cleavage enhancement observed is due to an increase in the overall affinity of these metallopeptides for a B-form substrate, through an alteration of their DNA site selectivity, or whether their effect(s) are more subtle such as an influence on DNA cleavage through an advantageous positioning of the active oxidizing moiety of the metallopeptide relative to a deoxyribose C−H target. In light of the above and given that Xaa-Xaa-His peptides are known to bind to metal ions with little influence from the side chains of the amino acids they contain (*2*), it can seemingly be ruled out that the differing activities observed are due to an influence on the overall metal binding properties of these tripeptides; amino acid substitutions with side chains bulkier than glycine within the Xaa-Xaa-His tripeptide have shown little effect on metal complexation at or above physiological pH values (*2*). Indeed, metal ion titrations indicate (Supporting Information) the formation of 1:1 Ni(II)·peptide complexes with all members of the Ni(II)·Oaa_1-Xaa-His and Ni(II)·Xaa-Oaa_2-His libraries except for Xaa-Pro-His; as expected, the substitution of Pro within the second peptide position prevents metal binding and subsequent DNA cleavage due to the lack of an amide bond necessary for metal ion complexation (*2*).

Table 1: DNA Binding Affinities of Selected Ni(II)·Xaa-Xaa-His Metallopeptides[a]

metallopeptide	binding affinity (M^{-1})
Ni(II)·Gly-Gly-His	3.9×10^7
Ni(II)·Lys-Gly-His	7.0×10^7
Ni(II)·Pro-Gly-His	7.4×10^7
Ni(II)·Pro-Ser-His	1.5×10^8
Ni(II)·Pro-Lys-His	1.4×10^8
distamycin (*29*)	1.0×10^8

[a] DNA binding affinities were determined as outlined in the Experimental Procedures.

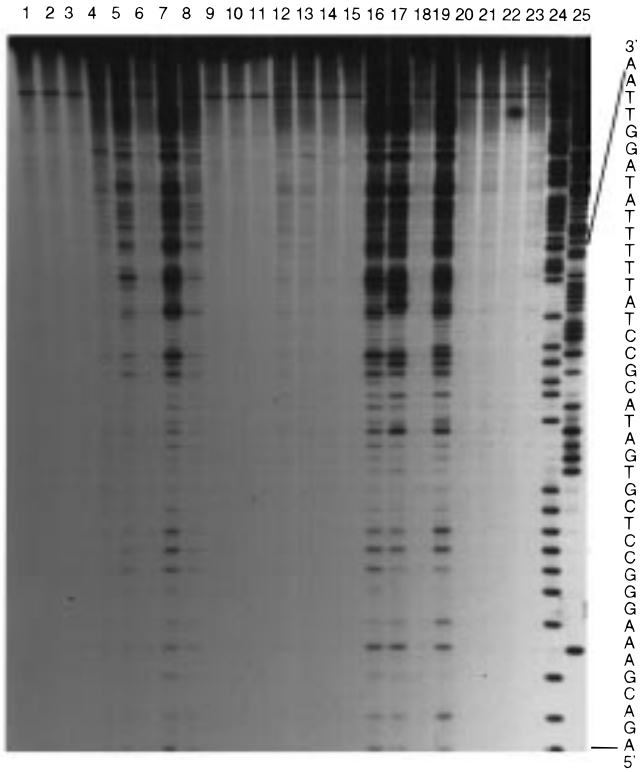

FIGURE 3: Autoradiogram of a high-resolution denaturing polyacrylamide gel analyzing 10 μM Ni(II)·Oaa$_1$-Xaa-His/$KHSO_5$-induced DNA cleavage of a 5′-^{32}P-end-labeled restriction fragment as described in Experimental Procedures: lane 1, intact DNA; lane 2, reaction control (10 μM Ni(II)·Gly-Gly-His alone); lane 3, reaction control (10 μM Ni(II)/$KHSO_5$); lane 4, 10 μM Ni(II)·Gly-Gly-His/$KHSO_5$; lane 5, 10 μM Ni(II)·Lys-Gly-His/$KHSO_5$; lane 6, Ni(II)·Ala-Xaa-His; lane 7, Ni(II)·Arg-Xaa-His; lane 8, Ni(II)·Asn-Xaa-His; lane 9, Ni(II)·Asp-Xaa-His; lane 10, Ni(II)·Gln-Xaa-His; lane 11, Ni(II)·Glu-Xaa-His; lane 12, Ni(II)·Gly-Xaa-His; lane 13, Ni(II)·His-Xaa-His; lane 14, Ni(II)·Ile-Xaa-His; lane 15, Ni(II)·Leu-Xaa-His; lane 16, Ni(II)·Lys-Xaa-His; lane 17, Ni(II)·Met-Xaa-His; lane 18, Ni(II)·Phe-Xaa-His; lane 19, Ni(II)·Pro-Xaa-His; lane 20, Ni(II)·Ser-Xaa-His; lane 21, Ni(II)·Thr-Xaa-His; lane 22, Ni(II)·Tyr-Xaa-His; lane 23, Ni(II)·Val-Xaa-His; lanes 24 and 25, Maxam−Gilbert A + G and T + C base-specific sequencing reactions, respectively.

Examination of Ni(II)·Oaa$_1$-Xaa-His and Ni(II)·Xaa-Oaa$_2$-His DNA Binding Affinity, Site Selectivity, and Cleavage Mechanism. To examine whether the increased activity of the above metallopeptides is due to an increase in their overall affinities for a B-form DNA substrate, we determined the binding affinities of selected metallotripeptides (Supporting Information). As shown in Table 1, the DNA binding affinities, as examined through a distamycin competition assay (*17, 28*), of the selected metallotripeptides were found to be very similar within a factor of 2−4 in most instances

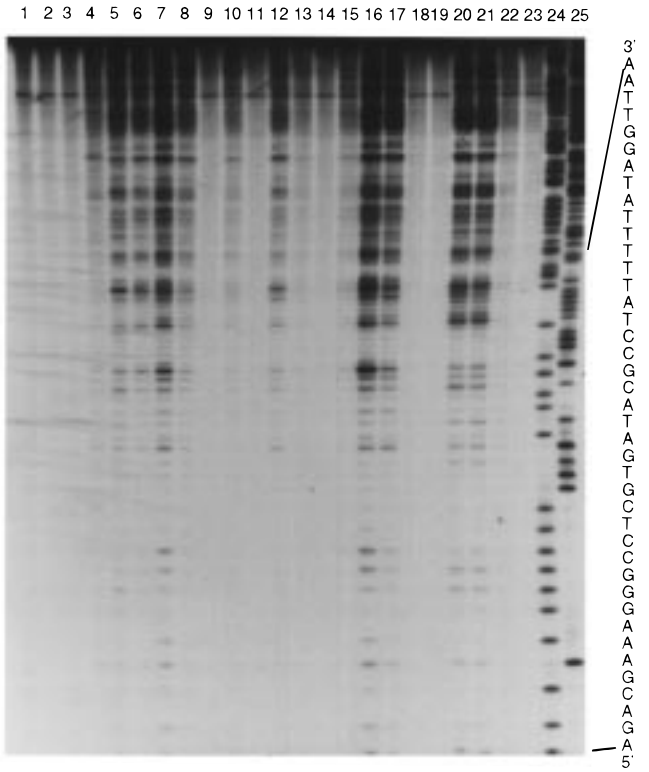

FIGURE 4: Autoradiogram of a high-resolution denaturing polyacrylamide gel analyzing 10 μM Ni(II)·Xaa-Oaa$_2$-His/$KHSO_5$-metallopeptide-induced DNA cleavage of a 5′-^{32}P-end-labeled restriction fragment as described in Experimental Procedures: lane 1, intact DNA; lane 2, reaction control (10 μM Ni(II)·Gly-Gly-His alone); lane 3, reaction control (10 μM Ni(II)/$KHSO_5$); lane 4, 10 μM Ni(II)·Gly-Gly-His/$KHSO_5$; lane 5, 10 μM Ni(II)·Lys-Gly-His/$KHSO_5$; lane 6, Ni(II)·Xaa-Ala-His; lane 7, Ni(II)·Xaa-Arg-His; lane 8, Ni(II)·Xaa-Asn-His; lane 9, Ni(II)·Xaa-Asp-His; lane 10, Ni(II)·Xaa-Gln-His; lane 11, Ni(II)·Xaa-Glu-His; lane 12, Ni(II)·Xaa-Gly-His; lane 13, Ni(II)·Xaa-His-His; lane 14, Ni(II)·Xaa-Ile-His; lane 15, Ni(II)·Xaa-Leu-His; lane 16, Ni(II)·Xaa-Lys-His; lane 17, Ni(II)·Xaa-Met-His; lane 18, Ni(II)·Xaa-Phe-His; lane 19, Ni(II)·Xaa-Pro-His; lane 20, Ni(II)·Xaa-Ser-His; lane 21, Ni(II)·Xaa-Thr-His; lane 22, Ni(II)·Xaa-Tyr-His; lane 23, Ni(II)·Xaa-Val-His; lanes 24 and 25, Maxam−Gilbert A + G and T + C base-specific sequencing reactions, respectively.

in comparison to Ni(II)·Gly-Gly-His. Given that the observed cleavage enhancements were up to 10-fold, these results suggest that structural features of the selected metallopeptides, in addition to their equilibrium binding, serve to influence their DNA cleavage enhancement.

Along with examining their overall DNA affinities, site-selective DNA cleavage by the libraries was also examined using end-labeled restriction fragments and high-resolution polyacrylamide gel analyses. As shown in Figures 3 and 4, all amino acid substitutions that resulted in an increase in DNA cleavage activity maintained a similar preference for A/T-rich DNA regions, albeit with some slight differences in selectivity (Figure 3, lanes 16 vs 17), and exhibited cleavage efficiencies that paralleled the results obtained with the plasmid cleavage assay. This selectivity is further emphasized in Figure 5 which illustrates the cleavage of both complementary DNA restriction fragment strands by Ni(II)·Pro-Xaa-His and Ni(II)·Xaa-Lys-His, the two most efficient peptide families generated; similar results were also obtained with the Ni(II)·Pro-Lys-His optimized metallopeptide. Figure 5 also emphasizes the 3′-asymmetry associated with DNA cleavage by the metallopeptides indicating a minor groove

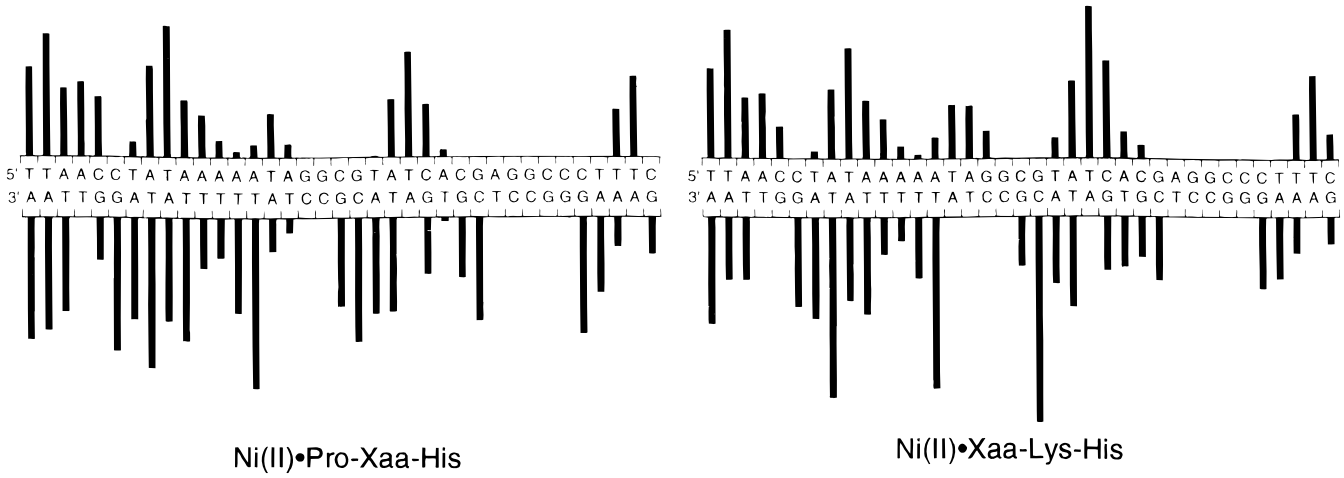

FIGURE 5: Histogram generated from the densitometric analysis of DNA cleavage of both complementary strands of a restriction fragment by Ni(II)·Pro-Xaa-His (left) and Ni(II)·Xaa-Lys-His (right). This depiction emphasizes the similarities in their A/T-rich cleavage selectivities and the associated 3′-asymmetry of their cleavage patterns.

association (*1*), as also observed in other studies (*17*). These observations are in accordance with previous studies which indicated that peptides including D-amino acids, especially in the second peptide position, resulted in altered selectivities while peptides containing all L-α amino acids exhibit A/T selectivity (*17*).

In addition to revealing their overall site selectivity, these experiments also indicate that the mechanism of DNA cleavage remains unaltered with changes to the basic metallopeptide framework; the products formed are wholly consistent with a C4′-H abstraction mechanism documented in earlier studies (*19*). As observed previously, direct DNA strand scission occurs without a subsequent chemical workup (i.e., piperidine treatment), and cleavage products containing phosphate termini and glycolate termini are observed. These results strongly suggest that some common element of the basic Ni(II)·Xaa-Xaa-His framework leads to the observed A/T selectivity and that the combinatorially selected enhancements increase metallopeptide activity through the presentation of a complementary series of noncovalent interactions with the minor groove of a DNA substrate which facilitate C4′-H abstraction.

Molecular Modeling. To examine the possible basis for the increased activity of the selected metallopeptides, we performed molecular modeling studies using the peptide with the highest selected activity, Ni(II)·Pro-Lys-His. Given that the most prominent feature of the common metallopeptide framework that supports A/T selectivity is the imidazole ring, models were constructed in which the N3 hydrogen of the imidazole acts as a hydrogen bond donor to the most prominent hydrogen bond acceptors found at the floor of the minor groove of A/T-rich regions, the exocyclic O2 of thymine, or the N3 of adenine (*33*). Two lines of evidence indirectly and directly, respectively, support the notion of a hydrogen bond between this portion of the metallopeptide framework and the floor of the minor groove: (1) it is well-documented that metal complexes of imidazoles increase the acidity of the pyrrole nitrogen of the imidazole ring (*34*) thus making it a very good hydrogen bond donor functionality which is present in all of the metallopeptides studied and (2) Ni(II) complexes of synthetic Xaa-Xaa-His tripeptides containing a His N3 methyl substituent do not cleave DNA suggesting that the elimination of this metallopeptide hydrogen bond functionality can prevent metallopeptide−DNA minor groove association (*35*).

Close examination of molecular models of Ni(II)·Pro-Lys-His bound to an A/T-rich region of B-form DNA (Supporting Information) indicates that with the imidazole nitrogen hydrogen-bonded to either the N3 of adenine or the O2 of thymine, the proline β, γ, and δ carbons are positioned deeply in the minor groove and poised to make van der Waals contacts with the deoxyribose sugars which form the walls of this groove. In addition, the Lys side chain contained within the second position of the metallopeptide framework is positioned such that this ionic residue is exposed to solvent and capable of forming van der Waals contacts with the edges of the deoxyribose rings and also a salt bridge with a phosphate group proximal to the bound metallopeptide; modeling also suggests that the side-chain hydroxyl functionalities of Ser or Thr residues are similarly capable of interacting with a phosphate proximal to the bound metallopeptide.

These models suggest that the first position of the metallopeptide is inserted into the minor groove and can be most effectively stabilized through hydrophobic contacts (via Pro or Met residues) and the second position is mostly influenced by either ionic (Lys/Arg) or polar (Ser/Thr) residues. With the metallopeptide situated as described above, the metal center is poised to interact (3−4 Å) with a readily accessible C4′-H leading to the observed cleavage products.

Summary. Direct deoxyribose-based strand scission of B-form DNA by Ni(II)·Xaa-Xaa-His metallopeptides can be enhanced up to an order of magnitude beyond the activity of Ni(II)·Gly-Gly-His through the inclusion of a hydrophobic amino acid (Pro/Met) in the amino-terminal position and an ionic (Lys/Arg) or polar (Thr/Ser) residue in the second position of the tripeptide ligand. While these substitutions can slightly increase metallopeptide−DNA affinity without significant changes in site selectivity, the increased reactivity observed likely benefits from the anchoring and proximity of the activated metallopeptide relative to its target C4′-H bond through noncovalent peptide−DNA contacts, as supported by molecular modeling studies. This information, and the combinatorial procedures described, could assist in the

further use of metallopeptides in developing metal-based nucleic acid targeted agents with increased activities or assist in the rational design or redesign of naturally occurring antitumor agents. In addition, the selection of amino acids known to be included in naturally occurring minor groove binding protein motifs suggests that Ni(II)·Xaa-Xaa-His metallopeptides can further our understanding of minor groove−amino acid/peptide recognition phenomena.

ACKNOWLEDGMENT

We would like to thank Dr. William L. Scott, Eli Lilly & Co., for the use of equipment necessary to generate synthetic peptide libraries.

SUPPORTING INFORMATION AVAILABLE

Agarose gel analyses of DNA plasmid cleavage by the metallopeptide libraries, visible absorption spectra of Cu(II)·Pro-Gly-His and Ni(II)·Pro-Gly-His, examples of metal ion titrations with the Oaa_1-Xaa-His and Xaa-Oaa_2−His libraries, examples of agarose gel analyses for the determination of DNA binding affinities through distamycin competition, and a molecular model of Ni(II)·Pro-Lys-His bound to DNA. This material is available free of charge via the Internet at http://pubs.acs.org.

REFERENCES

1. Dervan, P. B. (1991) *Methods Enzymol. 208*, 497−515.
2. Harford, C., and Sarkar, B. (1997) *Acc. Chem. Res. 30*, 123−130.
3. Long, E. C., Eason, P. D., and Liang, Q. (1996) *Met. Ions Biol. Syst. 33*, 427−452.
4. Shullenberger, D. F., Eason, P. D., and Long, E. C. (1993) *J. Am. Chem. Soc. 115*, 11038−11039.
5. Nagaoka, M., Hagihara, M., Kuwahara, J., and Sugiura, Y. (1994) *J. Am. Chem. Soc. 116*, 4085−4086.
6. Mack, D. P., Iverson, B. L., and Dervan, P. B. (1988) *J. Am. Chem. Soc. 110*, 7572−7574.
7. Mack, D. P., and Dervan, P. B. (1990) *J. Am. Chem. Soc. 112*, 4604−4606.
8. Mack, D. P., and Dervan, P. B. (1992) *Biochemistry 31*, 9399−9405.
9. Harford, C., Narindrasorasak, S., and Sarkar, B. (1996) *Biochemistry 35*, 4271−4278.
10. Footer, M., Egholm, M., Kron, S., Coull, J. M., and Matsudaira, P. (1996) *Biochemistry 35*, 10673−10679.
11. Brown, K., Yang, S.-H., and Kodadek, T. (1995) *Biochemistry 34*, 4733−4739.
12. Bertrand, R., Derancourt, J., and Kassab, R. (1997) *Biochemistry 36*, 9703−9714.
13. Brown, K. C., Yu, Z., Burlingame, A. L., and Craik, C. S. (1998) *Biochemistry 37*, 4397−4406.
14. Cuenoud, B., Tarasow, T. M., and Schepartz, A. (1992) *Tetrahedron Lett. 33*, 895−898.
15. Shullenberger, D. F., and Long, E. C. (1993) *Bioorg. Med. Chem. Lett. 3*, 333−336.
16. Grokhovsky, S. L., Nikolaev, V. A., Zubarev, V. E., Surovaya, A. N., Zhuze, A. L., Chernov, B. K., Sidorova, N., and Zasedatelev, A. S. (1992) *Mol. Biol. (Moscow) 26*, 1274−1297.
17. Liang, Q., Eason, P. D., and Long, E. C. (1995) *J. Am. Chem. Soc. 117*, 9625−9631.
18. Ananias, D. C., and Long, E. C. (1997) *Inorg. Chem. 36*, 2469−2471.
19. Liang, Q., Ananias, D. C., and Long, E. C. (1998) *J. Am. Chem. Soc. 120*, 248−257.
20. Muller, J. G., Hickerson, R. P., Perez, R. J., and Burrows, C. J. (1997) *J. Am. Chem. Soc. 119*, 1501−1506.
21. Brittain, I. J., Huang, X., and Long, E. C. (1998) *Biochemistry 37*, 12113−12120.
22. Dooley, C. T., and Houghten, R. A. (1993) *Life Sci. 52*, 1509−1517.
23. Houghten, R. A., Pinilla, C., Blondelle, S. E., Appel, J. R., Dooley, C. T., and Cuervo, J. H. (1991) *Nature 354*, 84−86.
24. Stewart, J. M., and Young, J. D. (1984) *Solid-Phase Peptide Synthesis*, Pierce Chemical Co., Rockford, IL.
25. Scott, W. L., Zhou, C., Fang, Z., and O'Donnell, M. J. (1997) *Tetrahedron Lett. 38*, 3695−3698.
26. Bernadou, J., Pratviel, G., Bennis, F., Giradet, M., and Meunier, B. (1989) *Biochemistry 28*, 7268−7275.
27. Maniatis, T., Fritsch, E. F., and Sambrook, J. (1982) *Molecular Cloning*, Cold Spring Harbor Laboratory, New York.
28. Brenowitz, M., Senear, D. F., Shea, M. A., and Ackers, G. K. (1986) *Methods Enzymol. 130*, 133−181.
29. Zimmer, C., and Wahnert, U. (1986) *Prog. Biophys. Mol. Biol. 47*, 31−112.
30. Camerman, N., Camerman, A., and Sarkar, B. (1976) *Can. J. Chem. 54*, 1309−1316.
31. Sheardy, R. D., Wilson, W. D., and King, H. D. (1989) in *Chemistry and Physics of DNA-Ligand Interactions* (Kallenbach, N. R., Ed.) pp 175−212, Adenine Press, Albany, NY.
32. Suzuki, M. (1989) *EMBO J. 8*, 797−804.
33. Kielkopf, C. L., White, S., Szewczyk, J. W., Turner, J. M., Baird, E. E., Dervan, P. B., and Rees, D. C. (1998) *Science 282*, 111−115.
34. Sundberg, R. J., and Martin, R. B. (1974) *Chem. Rev. 74*, 471−517.
35. Eason, P. D. (1997) Ph.D. Dissertation, Purdue University.

BI982587O